

Efficient Numerical Evaluation of Feynman Integral

Zhao Li,^{1,2,*} Jian Wang,^{3,†} Qi-Shu Yan,^{4,5,‡} and Xiaoran Zhao^{1,4,§}

¹*Institute of High Energy Physics, Chinese Academy of Sciences, Beijing 100049, P.R. China*

²*State Key Laboratory of Theoretical Physics, Institute of Theoretical Physics,
Chinese Academy of Sciences, Beijing 100190, P.R. China*

³*PRISMA Cluster of Excellence & Mainz Institute for Theoretical Physics,
Johannes Gutenberg University, D-55099 Mainz, Germany*

⁴*School of Physics Sciences, University of Chinese Academy of Sciences, Beijing 100049, P.R. China*

⁵*Center for High-Energy Physics, Peking University, Beijing, 100871, P.R. China*

Feynman loop integral is the key ingredient of high order radiation effect, which is responsible for reliable and accurate theoretical prediction. We improve the efficiency of numerical integration in sector decomposition by implementing quasi-Monte Carlo method associated with the technique of CUDA/GPU. For demonstration we present the results of several Feynman integrals up to two loops in both Euclidean and physical kinematic regions in comparison with those obtained from FIESTA3. It is shown that both planar and non-planar two-loop master integrals in physical kinematic region can be evaluated in less than half minute with $\mathcal{O}(10^{-3})$ accuracy, which makes the direct numerical approach viable for the precise investigation on the high order effect in multi-loop processes, e.g. the next-to-leading order QCD effect in Higgs pair production via gluon fusion with finite top quark mass.

PACS numbers: 02.60.Jh, 12.38.Bx, 14.80.Bn

Keywords: sector decomposition, quasi-Monte Carlo, Higgs

I. INTRODUCTION

The scalar particle predicted by the Standard Model, Higgs boson, has been eventually discovered at the CERN Large Hadron Collider (LHC)[1, 2]. This milestone inspires various exciting investigations on the further details of Higgs boson and related researches. Recently the launch of LHC RunII at 13 TeV collision energy brings physics exploration to a new era. With the highest center-of-mass energy and highest luminosity, many scattering processes that potentially answer some fundamental physics questions will be able to reach the accuracy in percent range or better, while the appropriate analysis on the high precision data demands that the uncertainties of theoretical prediction reach the same accuracy. In order to achieve this, high order QCD effect must be included in theoretical predictions. For instance, the state-of-the-art investigations on the Higgs inclusive production have explored next-to-next-to-leading order (NNNLO) effect for quark pair annihilation initial state [3] and for gluon fusion initial state [4]. Meanwhile the next-to-next-to-leading order (NNLO) theoretical predictions have been provided for the Higgs pair production [5] and the associated production of Higgs with jet[6–8] or vector boson [9–12]. As the increase of accumulated luminosity at LHC, the investigation on high order QCD effect will be wanted for more processes, e.g. top quark production and jet cross sections. In the high order effect, one of the most important ingredients is the virtual correction, which always relies on evaluation of Feynman loop integrals.

After decades of effort, various algorithms have been proposed for evaluating Feynman loop integral including both analytical and numerical approaches. The analytical approaches can provide the explicit expression for the Feynman integral, and can further reveal significant physical characteristics. However when complicated processes are encountered, it becomes difficult to obtain analytical solutions, while the numerical approaches can solve more challenging problems in spite of heavy burden of evaluation time. Sector decomposition, one of the numerical algorithms, was introduced as a systematic approach by Binoth and Heinrich[13, 14]. Following certain choice of decomposition strategies, this algorithm divides the domain of loop integration into sectors. In each individual sector proper transformation of integration variables is performed to explicitly reveal the ultraviolet (UV) and infrared (IR) singularities. Ultimately the coefficients of Laurent series in ϵ of Feynman integral can be evaluated numerically. Initially sector decomposition was implemented for the Feynman integral in Euclidean kinematic region[13–15], where the Cauchy

*Electronic address: zhaoli@ihep.ac.cn

†Electronic address: jian.wang@uni-mainz.de

‡Electronic address: yanqishu@ucas.ac.cn

§Electronic address: zhaoxiaoran13@mails.ucas.ac.cn

singular integral can be avoid. Later inspired by Nagy and Soper[16, 17], integration contour deformation is proposed [18] as a systematic scheme to extend sector decomposition to physical kinematic region.

Several programs [19–21] have implemented the sector decomposition algorithm for the numerical evaluation of Feynman loop integrals. Normally they use Monte Carlo (MC) integration methods, which have been widely used in high energy physics research. For instance, Vegas[22], an adaptive Monte Carlo method, can achieve the integration convergence rate of $\mathcal{O}(1/\sqrt{n})$. In this paper, we implement the quasi-Monte Carlo (QMC) method to the numerical evaluation of the integrals in sector decomposition. As a better choice, QMC can have a convergence rate close to $\mathcal{O}(n^{-1})$ for differentiable integrand. Furthermore, we adopt the technique of CUDA/GPU to improve the performance of numerical evaluation.

This paper is organised as follows: In Section II we review the sector decomposition algorithm. Section III gives a brief description of the QMC integration method. In Section IV we compare the performance of our program with FIESTA[20]. Then conclusion is presented in the final section.

II. SECTOR DECOMPOSITION

Generically an L -loop Feynman integral has the following representation.

$$I = \int \left(\prod_{l=1}^L \frac{d^D k_l}{i\pi^{\frac{D}{2}}} \right) \prod_{j=1}^N \frac{1}{(q_j^2 - m_j^2 + i\varepsilon)^{\nu_j}}, \quad (1)$$

where $D = 4 - 2\epsilon$. q_j is the momentum of relevant internal propagator, and is linear combination of the loop momenta $\{k_l\}$ and external momenta. m_j is the mass of relevant internal propagator. ν_j is the power of the corresponding propagator.

After Feynman parameterisation and integration over loop momenta, one can obtain

$$I = (-1)^{N_\nu} \frac{\Gamma(N_\nu - LD/2)}{\prod_{j=1}^N \Gamma(\nu_j)} \int_0^\infty \cdots \int_0^\infty \left(\prod_{l=1}^N dx_l x_l^{\nu_l-1} \right) \delta \left(1 - \sum_{l=1}^N x_l \right) \frac{U^{N_\nu - (L+1)D/2}(x_1, \dots, x_N)}{F^{N_\nu - LD/2}(x_1, \dots, x_N)}, \quad (2)$$

where $N_\nu = \sum_{j=1}^N \nu_j$. U and F are polynomials of $\{x_l\}$ and can be straightforwardly derived from the momentum representation, or constructed from the topology of the corresponding Feynman graph [23].

Further treatment on Feynman integral requires careful consideration since U and F can vanish when some of $\{x_l\}$ approach zero, which may be related to UV or IR divergence. Direct numerical integration is impossible for divergent integrals. Sector decomposition algorithm is designed to systematically extract the divergence, and is briefly described as follows[24].

Firstly, the integration domain is equally split into N sub-domains, which are called primary sectors:

$$\int_0^\infty d^N x = \sum_i^N \int_0^\infty d^N x \prod_{\substack{j=1 \\ j \neq i}}^N \theta(x_i - x_j). \quad (3)$$

Then in the i -th sector we implement the variable transformation,

$$x_j = \begin{cases} x_i t_j & j < i, \\ x_i & j = i, \\ x_i t_{j-1} & j > i. \end{cases} \quad (4)$$

Thereafter x_i integration is performed associated with the step function, and now the Feynman integral can be expressed as

$$I = (-1)^{N_\nu} \frac{\Gamma(N_\nu - LD/2)}{\prod_{j=1}^N \Gamma(\nu_j)} \sum_l^N I_l, \quad (5)$$

where

$$I_l = \int_0^1 \cdots \int_0^1 \left(\prod_{j=1}^{N-1} dt_j t_j^{\nu_j-1} \right) \frac{U_l^{N_\nu - (L+1)D/2}(t_1, \dots, t_{N-1})}{F_l^{N_\nu - LD/2}(t_1, \dots, t_{N-1})}. \quad (6)$$

Obviously for any given primary sector I_l , the domain of integration is $(N - 1)$ -dimensional unit cube.

Next, following iterative decomposition strategy[19] or geometric strategy [25, 26], each primary sector is finally divided into some subsectors $\{I_{la}\}$ so that in any subsector polynomials U_l and F_l can be factorised into the form

$$U_l = C_{la}(1 + H_{la}(t_1, \dots, t_{N-1})) \prod_{j=0}^{N-1} t_j^{b_{la,j}} \quad (7)$$

$$F_l = C'_{la}(1 + H'_{la}(t_1, \dots, t_{N-1})) \prod_{j=0}^{N-1} t_j^{b'_{la,j}} \quad (8)$$

$$(9)$$

after proper variable transformation. In each subsector, the new variables and Jacobian generated by the transformation are required to be monomials of original variables, and meanwhile the transformation projects the domain of integration to $(N - 1)$ -dimensional unit cube. In above expressions, $b_{la,j}$ and $b'_{la,j}$ are non-negative integers. H_{la} and H'_{la} are polynomials of $\{t_j\}$ such that $H_{la}(0, \dots, 0) = 0$ and $H'_{la}(0, \dots, 0) = 0$.

Now the primary sector becomes the combination of subsectors,

$$I_l = \sum_{a=1}^m D_{la} \int_0^1 \cdots \int_0^1 \left(\prod_{j=1}^{N-1} dt_j t_j^{\alpha_{la,j} + \beta_{la,j}\epsilon} \right) \frac{(1 + H_{la}(t_1, \dots, t_{N-1}))^{N_\nu - (L+1)D/2}}{(1 + H'_{la}(t_1, \dots, t_{N-1}))^{N_\nu - LD/2}}, \quad (10)$$

where the powers of t_j are collected into $\alpha_{la,j} + \beta_{la,j}\epsilon$, and D_{la} contains the coefficients from Jacobian and C_{la} and C'_{la} .

In the practical evaluation of Feynman integrals, we will adopt the geometric strategy since it can be guaranteed to succeed and results in the smallest number of subsectors.

After sector decomposition, the singularities in the Feynman integral have been collected into the regulators in form of $t^{\alpha+\beta\epsilon}$, which can explicitly present the pole of the integral by using Laurent series or integration by parts (IBP). Without loss of generality, we rewrite the integral with certain regulator as

$$\mathcal{I} = \int_0^1 dt t^{\alpha+\beta\epsilon} f(t, \epsilon), \quad (11)$$

where $f(0, \epsilon)$ is non-zero finite. Then if $\alpha \leq -1$, the above integral contains singularity on the lower bound. By expanding $f(t, \epsilon)$ into a Laurent series around $t = 0$, the singularity can be explicitly extracted as

$$\mathcal{I} = \sum_{p=0}^{|\alpha|-1} \frac{1}{\alpha + p + 1 + \beta\epsilon} \frac{f^{(p)}(0, \epsilon)}{p!} + \int_0^1 dt t^{\alpha+\beta\epsilon} r(t, \epsilon), \quad (12)$$

where

$$r(t, \epsilon) = f(t, \epsilon) - \sum_{p=0}^{|\alpha|-1} f^{(p)}(0, \epsilon) \frac{t^p}{p!}. \quad (13)$$

Thereafter, the integrands can be expanded by small ϵ , and the coefficients of Laurent series in ϵ can be evaluated numerically order by order. However, numerical evaluation of $r(t)$ may suffer numerical instability from large number cancellation. An alternative approach to the pole extraction that can avoid this problem is IBP,

$$\int_0^1 dt t^{\alpha+\beta\epsilon} f(t, \epsilon) = \frac{1}{\alpha + \beta\epsilon + 1} f(1, \epsilon) - \int_0^1 dt \frac{\partial f(t, \epsilon)}{\partial t} \frac{t^{\alpha+\beta\epsilon+1}}{\alpha + \beta\epsilon + 1}. \quad (14)$$

It can be seen that the power of t increases by one. Therefore, by repeating the above IBP formula enough times, the power of t will not generate singularity, and then the numerical approach can be implemented to evaluate the coefficients of Laurent series in ϵ .

However, occasionally the integral contains Cauchy singularities in physical kinematic region. In this case, the sign of F cannot be guaranteed definite, so the Cauchy singular Feynman integral is only valid under a proper contour according to the conventional $i\epsilon$ prescription of the Feynman propagators. Practically such infinitesimal shifted contour

will sabotage the stability of numerical integration. Fortunately an interesting prescription of contour deformation has been proposed [18]

$$z_i(\vec{t}) = t_i - i\lambda_i t_i(1 - t_i) \frac{\partial F(\vec{t})}{\partial t_i}, \quad (15)$$

where an appropriate choice of λ_i can guarantee the sign of $\text{Im}(F(\vec{z}))$ always negative as required conventionally.

III. QUASI-MONTE CARLO

After the implementation of the sector decomposition algorithm reviewed in Section II, the Feynman integral is expressed as Laurent series in ϵ . Coefficients of the series are composed of convergent integrals, which can be numerically evaluated. One-dimensional integral can be easily evaluated by numerical approach such as trapezoidal rule, while numerical evaluation of multi-dimensional integral is commonly much more difficult.

For instance, a s -dimensional integral can be written as

$$I_s(f) = \int_{[0,1]^s} d^s x f(\vec{x}). \quad (16)$$

Given a predefined set of n points $\{\vec{x}_i | \vec{x}_i \in [0,1]^s; i = 0, \dots, n-1\}$, the above integral can be estimated by

$$Q_{n,s}(f) = \frac{1}{n} \sum_{i=0}^{n-1} f(\vec{x}_i) \approx I_s(f). \quad (17)$$

This method is called quasi-Monte Carlo method, and the point set is called quasi-Monte Carlo rule[27]. Conventionally two families of QMC rules attract most of interest. One is consist of digital nets and digital sequences, while the other is lattice rule. In this paper we adopt the rank-1 lattice rule (R1LR) defined by[27]

$$\vec{x}_i = \left\{ \frac{i\vec{z}}{n} \right\}, \quad i = 0, \dots, n-1, \quad (18)$$

where \vec{z} , known as the generating vector, is a s -dimensional integer vector. The integer components of \vec{z} are all relatively prime to n . The braces around the vector in the Eq. (18) means only the fractional part of each component in the vector is taken.

The previous R1LR will result in a biased estimation, since it is fully deterministic. To achieve unbiased result, we need to introduce appropriate randomisation. For R1LR, we can use the simplest form of randomisation called shifting, which will yield so-called shifted lattice rule. The QMC algorithm utilising random shifted R1LR is explained as below[27].

1. A set of m independent random vectors called shifts, $\{\vec{\Delta}_1, \dots, \vec{\Delta}_m\}$, is generated with uniform distribution in $[0,1]^s$.
2. For each shift, the integral estimation in Eq. (17) is repeated to obtain a set of m integral estimations, $\{Q_{n,s,1}(f), \dots, Q_{n,s,m}(f)\}$, where

$$Q_{n,s,k}(f) = \frac{1}{n} \sum_{i=0}^{n-1} f\left(\left\{ \frac{i\vec{z}}{n} + \vec{\Delta}_k \right\}\right), \quad k = 1, \dots, m. \quad (19)$$

3. Then the average of these m integral estimations

$$\bar{Q}_{n,s,m}(f) = \frac{1}{m} \sum_{k=1}^m Q_{n,s,k}(f) \quad (20)$$

is finally taken as an unbiased approximation of the integral $I_s(f)$.

4. Furthermore an unbiased estimation for the mean-square error of $\bar{Q}_{n,s,m}(f)$ can be obtained by

$$\frac{1}{m(m-1)} \sum_{k=1}^m (Q_{n,s,k}(f) - \bar{Q}_{n,s,m}(f))^2. \quad (21)$$

The above algorithm improves the practicability of R1LR QMC method. Moreover, in case that the integrand f is 1-periodic function and all partial derivatives of f exist, the convergence rate can be improved to $O(n^{-1})$ [28, 29] if the generating vector is obtained by the component-by-component construction. However, in practice even when the integrand f is non-periodic function, one can implement the transformation $x_i = 3y_i^2 - 2y_i^3$ to obtain periodic integrand as below.

$$I_s(f) = \int_{[0,1]^s} d^s x f(\vec{x}) = \int_{[0,1]^s} d^s y f(\vec{x}(\vec{y})) \prod_{i=1}^s (6y_i(1-y_i)) = \int_{[0,1]^s} d^s y g(\vec{y}), \quad (22)$$

where it can be seen that $g(\vec{y}) = 0$ once \vec{y} reaches boundary of $[0,1]^s$, as long as f is bounded at the edge.

Beside the $O(n^{-1})$ convergence rate, shifted R1LR QMC method has some intrinsic advantages. In shifted R1LR QMC method the lattice rule is deterministic and therefore the complexity of random number generation only depends on the number of shifts. By contrast in MC method, since the evaluation points are independent random vectors, large amount of pseudo random number generation consumes much more resource of GPU. Besides, since QMC method is non-adaptive method, it can easily deal with the integral in complex space, which is inevitable for Feynman integral in physical kinematic region. However, for the adaptive algorithms, e.g. Vegas, it is difficult to define an appropriate rule to handle such kind of integral.

IV. NUMERICAL RESULTS

In this section, we present some numerical results of several Feynman integrals up to two loops for certain choices of kinematic parameters as demonstration. In Euclidean kinematic region we show the evaluation of massless scalar double box diagrams. And in physical kinematic region we take several master integrals from the investigation of Higgs pair production via gluon fusion. The Higgs and top quark masses are chosen as $M_H = 125$ GeV and $M_t = 172$ GeV [30]. By comparing¹ with FIESTA3[20] using Vegas algorithm [22, 31] as benchmark of CPU efficiency, we illustrate the improvement on the efficiency of numerical evaluation of Feynman integral.

A. One-loop Feynman integral in physical kinematic region

The leading order (LO) contribution to Higgs pair production via gluon fusion contains the one-loop box Feynman diagram as shown in Fig. 1. For the evaluation of this diagram, the most complicated master integral is

$$I_A = \int \frac{d^D k}{(2\pi)^D} \frac{1}{(-k^2 + M_t^2 + i\varepsilon)[-(k+p_1)^2 + M_t^2 + i\varepsilon][-(k-p_2)^2 + M_t^2 + i\varepsilon][-(k+p_1-p_4)^2 + M_t^2 + i\varepsilon]}. \quad (23)$$

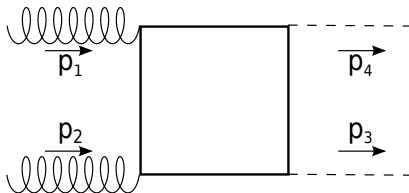


FIG. 1: One-loop box diagram for Higgs pair production via gluon fusion, where the initial state momenta are incoming and the final state momenta are outgoing.

The initial states are on-shell gluons $p_1^2 = p_2^2 = 0$, and the final states are on-shell Higgs bosons $p_3^2 = p_4^2 = M_H^2$. The Mandelstam variables are defined as $(p_1 + p_2)^2 = s$ and $(p_2 - p_3)^2 = t$.²

As shown in Fig.2, we evaluate 1000 points between $s = 70000$ and $s = 500000$, while $t = -6000$ is fixed. The average time of evaluating one point is 83ms, which is acceptable for practical calculation of one-loop Feynman integrals. We can found that the threshold effect is explicitly shown at $s = 4M_t^2 = 118336$. Below the threshold

¹ Our program was deployed with NVIDIA Tesla K20 GPU, while FIESTA3 used four cores of Intel Core i7 3770 CPU (3.4GHz).

² For simplicity, in the following the dimension of scale is set as GeV by default.

$\text{Re}(I_A)$ vanishes since at the moment the sign of F -term in each decomposed subsector is definite. Meanwhile $\text{Im}(I_A)$ peaks on the threshold, where we can see an obvious large relative error due to slow convergence of some integrals. Fig.2 also presents the comparison with results from LoopTools[32]. It can be seen that the relative errors of our results are within 10^{-3} , and the relative errors can be smaller than 10^{-4} for most of the points.

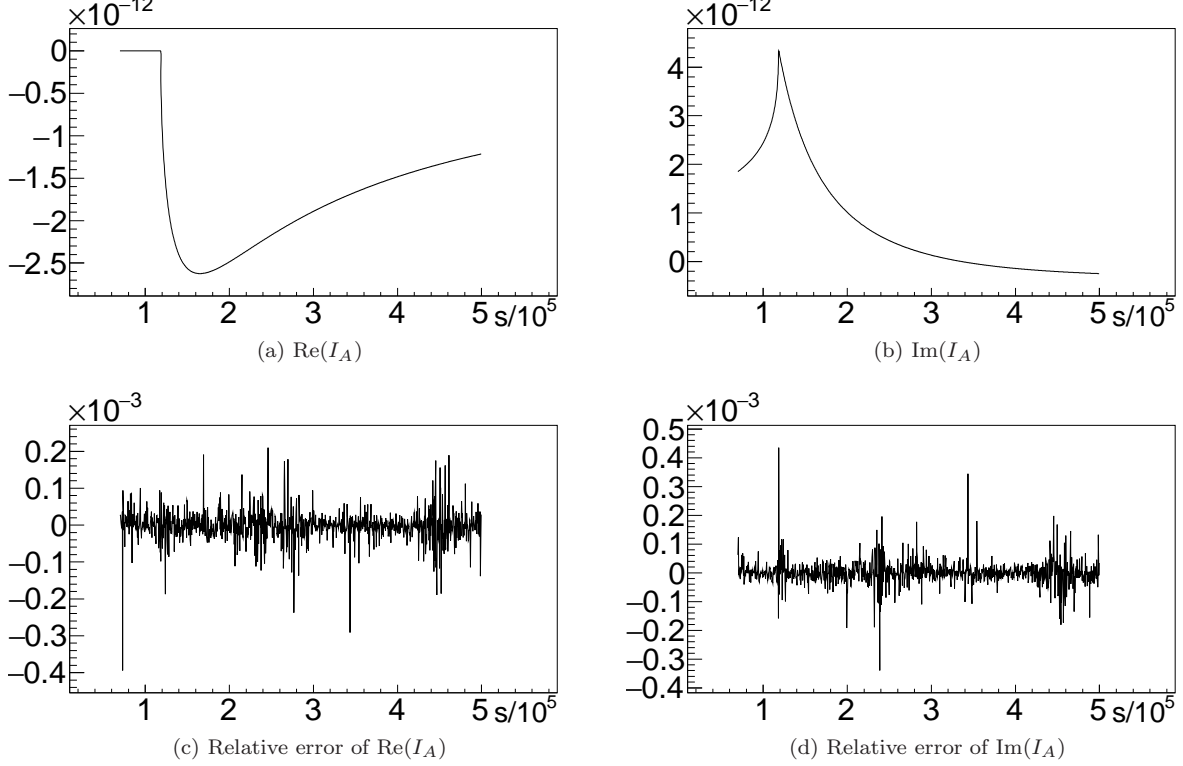


FIG. 2: Comparison of single box master integral with LoopTools.

B. Two-loop Feynman integral in Euclidean kinematic region

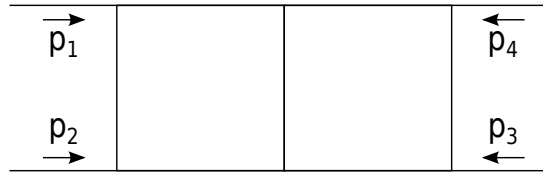


FIG. 3: Massless double box diagram with two legs off-shell [14], where all the external momenta are incoming.

For the demonstration of two-loop Feynman integral in Euclidean kinematic region, we choose the massless double box diagram with two legs off-shell [14], as shown in Fig. 3. Explicitly this Feynman integral is written as

$$I_B = \int \frac{d^D k_1}{i\pi^{\frac{D}{2}}} \frac{d^D k_2}{i\pi^{\frac{D}{2}}} \frac{1}{(-k_1^2 + i\varepsilon)[-(k_1 - p_1)^2 + i\varepsilon][-(k_1 + p_2)^2 + i\varepsilon]} \times \frac{1}{[-(k_1 - k_2 - p_1)^2 + i\varepsilon](-k_2^2 + i\varepsilon)[-(k_1 + p_2 - k_2 + p_3)^2 + i\varepsilon][-(k_1 - k_2 + p_2)^2 + i\varepsilon]}. \quad (24)$$

Because this Feynman integral contains divergences, the results are expressed in form of Laurent series in ϵ ,

$$I_B = e^{-2\epsilon\gamma_E} s^{-3-2\epsilon} \sum_{i=0}^{i=4} \frac{P_i}{\epsilon^i}. \quad (25)$$

During the numerical evaluation, the Mandelstam variables are set as $s = (p_1 + p_2)^2 = -2/3$, $t = (p_2 + p_3)^2 = -2/3$, and $u = (p_1 + p_3)^2 = -2/3$.

$(p_1^2, p_2^2, p_3^2, p_4^2)$	(-1,0,0,-1)		(0,-1,0,-1)		(0,0,-1,-1)	
	Vegas/CPU	QMC/GPU	Vegas/CPU	QMC/GPU	Vegas/CPU	QMC/GPU
P_4	$0.25 \pm 3 \times 10^{-6}$	$0.25 \pm 1 \times 10^{-7}$	0	0	0.2501 ± 0.0001	$0.25 \pm 2 \times 10^{-7}$
P_3	0.40547 ± 0.00004	0.40546 ± 0.00006	0	0	0.4057 ± 0.005	0.40544 ± 0.00003
P_2	0.6500 ± 0.0003	0.6489 ± 0.0005	1.0582 ± 0.0001	1.05799 ± 0.00003	3.118 ± 0.002	3.118 ± 0.001
P_1	-1.183 ± 0.001	-1.1823 ± 0.0006	1.0938 ± 0.0005	1.0947 ± 0.0009	12.522 ± 0.007	12.533 ± 0.007
P_0	-8.798 ± 0.004	-8.801 ± 0.005	-3.000 ± 0.001	-3.003 ± 0.002	35.60 ± 0.03	35.60 ± 0.03
Integration Time	500s	2.2s	45s	0.84s	117s	2.2s

TABLE I: Comparison of double box Feynman integral in Euclidean kinematic region.

In Table I, we compare our results (marked as QMC) with those from FIESTA3 [20]. It can be seen that the consistence of all the results is $\mathcal{O}(10^{-3})$, while our program is much (about 50-200 times) faster than FIESTA3. This implies that our program can provide the result of Feynman integral with much higher accuracy in Euclidean kinematic region.

C. Two-loop Feynman integral in physical kinematic region

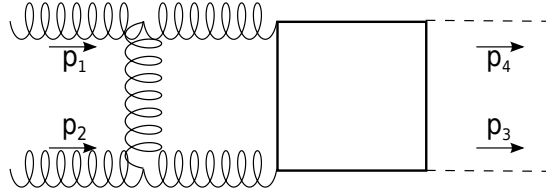


FIG. 4: Two-loop double box Feynman diagram for the Higgs pair production via gluon fusion, where the initial state momenta are incoming and the final state momenta are outgoing.

The next-to-leading order (NLO) contribution to Higgs pair production via gluon fusion contains the two-loop double box Feynman diagram as shown in Fig. 4, which is one of the challenges for analytical approach with finite top quark mass. To evaluate this diagram, we will confront the complicated master integral

$$I_C = \int \frac{d^D k_1}{i\pi^{\frac{D}{2}}} \frac{d^D k_2}{i\pi^{\frac{D}{2}}} \frac{1}{(-k_1^2 + i\varepsilon)[-(k_1 - p_1)^2 + i\varepsilon][-(k_1 + p_2)^2 + i\varepsilon][-(k_1 - k_2 - p_1)^2 + M_t^2 + i\varepsilon]} \times \frac{1}{(-k_2^2 + M_t^2 + i\varepsilon)[-(k_1 + p_2 - k_2 - p_3)^2 + M_t^2 + i\varepsilon][-(k_1 - k_2 + p_2)^2 + M_t^2 + i\varepsilon]}. \quad (26)$$

This Feynman integral contains IR divergences, so we express the results in form of Laurent series in ϵ ,

$$I_C = e^{-2\epsilon\gamma_E} s^{-3-2\epsilon} \sum_{i=0}^{i=2} \frac{P_i}{\epsilon^i}. \quad (27)$$

Here the initial states are on-shell gluons $p_1^2 = p_2^2 = 0$, and the final states are on-shell Higgs bosons $p_3^2 = p_4^2 = M_H^2$. The Mandelstam variables are set as $s = (p_1 + p_2)^2 = 160000$ and $t = (p_2 - p_3)^2 = -6000$.

	Vegas/CPU	QMC/GPU
P_2	$-7.959 \pm 0.009 - 10.586i \pm 0.009i$	$-7.949 \pm 0.003 - 10.585i \pm 0.005i$
P_1	$3.9 \pm 0.1 - 28.1i \pm 0.1i$	$3.831 \pm 0.005 - 28.022i \pm 0.005i$
P_0	$-3.9 \pm 0.8 + 92.3i \pm 0.8i$	$-4.63 \pm 0.07 + 92.13i \pm 0.07i$
Integration Time	45540s	19s

TABLE II: Comparison of two-loop double box Feynman integral in physical kinematic region.

As shown in Table II, after more than 12 hours, the relative error of finite term from FIESTA3 can only reach 10^{-2} . By comparison, in 19 seconds our program can obtain the accuracy about 10^{-3} , which may cost FIESTA3

more than thousand hours. Moreover, compared with the efficiency improvement obtained in Euclidean kinematic region in Section IV B, we can find a much better one in the physical kinematic region due to the advantages of QMC algorithm for complex integral as explained in Section III. Besides, it can be seen that the efficiency of our program for the two-loop Feynman integral makes the numerical approach viable for the evaluation of NLO virtual contribution to Higgs pair production via gluon fusion with finite top quark mass. Therefore the investigation on the finite top quark mass effect in the Higgs pair production can be accomplished in months.

D. Non-planar Two-loop Feynman integral in physical kinematic region

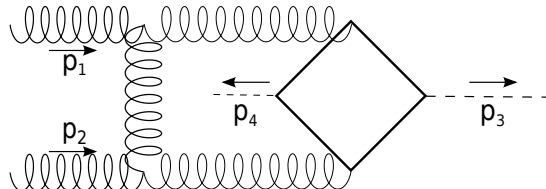


FIG. 5: Non-planar two-loop double box Feynman diagram for the Higgs pair production via gluon fusion, where the initial state momenta are incoming and the final state momenta are outgoing.

The non-planar two-loop diagram shown in Fig. 5 also contributes to Higgs pair production via gluon fusion at NLO. During the evaluation of this diagram, the most complicated master integral is

$$I_D = \int \frac{d^D k_1}{i\pi^{\frac{D}{2}}} \frac{d^D k_2}{i\pi^{\frac{D}{2}}} \frac{1}{(-k_1^2 + i\varepsilon)[-(k_1 + p_1)^2 + i\varepsilon][-(k_1 - p_2)^2 + i\varepsilon][-(k_1 + p_1 - k_2)^2 + M_t^2 + i\varepsilon]} \times \frac{1}{(-k_2^2 + M_t^2 + i\varepsilon)[-(k_2 - p_4)^2 + M_t^2 + i\varepsilon][-(k_1 + p_1 - k_2 - p_3)^2 + M_t^2 + i\varepsilon]}, \quad (28)$$

which contains IR divergences, and can be expressed in form of Laurent series in ϵ ,

$$I_D = e^{-2\epsilon\gamma_E} s^{-3-2\epsilon} \sum_{i=0}^{i=2} \frac{P_i}{\epsilon^i}. \quad (29)$$

Same as the configuration in Section IV C, the initial states are on-shell gluons $p_1^2 = p_2^2 = 0$, and the final states are on-shell Higgs bosons $p_3^2 = p_4^2 = M_H^2$. The Mandelstam variables are set as $s = (p_1 + p_2)^2 = 160000$ and $t = (p_2 - p_3)^2 = -6000$.

	Vegas/CPU	QMC/GPU
P_2	$-3.848 \pm 0.004 + 0.0005i \pm 0.003i$	$-3.8482 \pm 0.0007 + 0.0004i \pm 0.0003i$
P_1	$3.81 \pm 0.03 - 6.41i \pm 0.03i$	$3.83 \pm 0.02 - 6.40i \pm 0.02i$
P_0	$77.2 \pm 0.2 + 20.1i \pm 0.2i$	$77.2 \pm 0.1 + 19.9i \pm 0.1i$
Integration Time	54290s	20s

TABLE III: Comparison of non-planar two-loop double box Feynman integral in physical kinematic region.

In Table III, we can see that our program can obtain the result with $\mathcal{O}(10^{-3})$ accuracy in 20 seconds, while the relative error of FIESTA3 result can also reach almost the order accuracy after more than 15 hours. By comparing with the results in previous section, it is obvious that the non-planar double-box master integral has slower convergence rate. This is consistent with the conventional conclusion that the evaluation of non-planar diagram is more difficult than the planar one. Nonetheless, it can be seen that efficiency of our program for the evaluation of non-planar master integral is acceptable for the practical numerical approach, which can provide NLO numerical result for Higgs pair production in months.

V. CONCLUSION

We have implemented the shifted R1LR QMC method associated with CUDA/GPU to numerically evaluate Feynman loop integrals by using sector decomposition algorithm. Some examples are presented to show the promising

efficiency of our program on the numerical evaluation of Feynman loop integrals. For one-loop box Feynman integral, we could obtain accuracy about 10^{-4} in tens of milliseconds. And for two-loop double box Feynman integral, the accuracy can reach about 10^{-3} in several seconds in Euclidean kinematic region, while in physical kinematic region only less than half minute is needed. The efficiency of our program can make the direct numerical approach viable for the precise investigation on some important processes, e.g. Higgs pair production via gluon fusion at the NLO with the finite top quark mass effect.

Acknowledgments

This work was supported by the Natural Science Foundation of China under Grant No. 11305179 and No. 11475180; and by Youth Innovation Promotion Association, CAS; and by the IHEP Innovation Grant under contract number Y4545170Y2, and is partially supported by the State Key Lab for Electronics and Particle Detectors; and by the Open Project Program of State Key Laboratory of Theoretical Physics, Institute of Theoretical Physics, Chinese Academy of Sciences, China (No.Y4KF061CJ1); J.W. was supported by the Cluster of Excellence *Precision Physics, Fundamental Interactions and Structure of Matter* (PRISMA-EXC 1098).

-
- [1] G. Aad et al. (ATLAS), Phys.Lett. **B716**, 1 (2012), 1207.7214.
 - [2] S. Chatrchyan et al. (CMS), Phys.Lett. **B716**, 30 (2012), 1207.7235.
 - [3] C. Anzai, A. Hasselhuhn, M. Hschele, J. Hoff, W. Kilgore, et al. (2015), 1506.02674.
 - [4] C. Anastasiou, C. Duhr, F. Dulat, F. Herzog, and B. Mistlberger, Phys. Rev. Lett. **114**, 212001 (2015), 1503.06056.
 - [5] D. de Florian and J. Mazzitelli, Phys.Rev.Lett. **111**, 201801 (2013), 1309.6594.
 - [6] X. Chen, T. Gehrmann, E. Glover, and M. Jaquier, Phys.Lett. **B740**, 147 (2015), 1408.5325.
 - [7] R. Boughezal, F. Caola, K. Melnikov, F. Petriello, and M. Schulze (2015), 1504.07922.
 - [8] R. Boughezal, C. Focke, W. Giele, X. Liu, and F. Petriello, Phys. Lett. **B748**, 5 (2015), 1505.03893.
 - [9] O. Brein, A. Djouadi, and R. Harlander, Phys.Lett. **B579**, 149 (2004), hep-ph/0307206.
 - [10] O. Brein, R. Harlander, M. Wiesemann, and T. Zirke, Eur.Phys.J. **C72**, 1868 (2012), 1111.0761.
 - [11] G. Ferrera, M. Grazzini, and F. Tramontano, Phys. Rev. Lett. **107**, 152003 (2011), 1107.1164.
 - [12] G. Ferrera, M. Grazzini, and F. Tramontano, Phys. Lett. **B740**, 51 (2015), 1407.4747.
 - [13] T. Binoth and G. Heinrich, Nucl.Phys. **B585**, 741 (2000), hep-ph/0004013.
 - [14] T. Binoth and G. Heinrich, Nucl.Phys. **B680**, 375 (2004), hep-ph/0305234.
 - [15] G. Heinrich and V. A. Smirnov, Phys.Lett. **B598**, 55 (2004), hep-ph/0406053.
 - [16] Z. Nagy and D. E. Soper, JHEP **0309**, 055 (2003), hep-ph/0308127.
 - [17] Z. Nagy and D. E. Soper, Phys.Rev. **D74**, 093006 (2006), hep-ph/0610028.
 - [18] C. Anastasiou, S. Beerli, and A. Daleo, JHEP **0705**, 071 (2007), hep-ph/0703282.
 - [19] C. Bogner and S. Weinzierl, Comput.Phys.Comm. **178**, 596 (2008), 0709.4092.
 - [20] A. V. Smirnov, Comput.Phys.Comm. **185**, 2090 (2014), 1312.3186.
 - [21] S. Borowka, G. Heinrich, S. Jones, M. Kerner, J. Schlenk, et al. (2015), 1502.06595.
 - [22] G. P. Lepage (1980).
 - [23] C. Bogner and S. Weinzierl, Int.J.Mod.Phys. **A25**, 2585 (2010), 1002.3458.
 - [24] G. Heinrich, Int.J.Mod.Phys. **A23**, 1457 (2008), 0803.4177.
 - [25] T. Kaneko and T. Ueda, Comput.Phys.Comm. **181**, 1352 (2010), 0908.2897.
 - [26] T. Kaneko and T. Ueda, PoS **ACAT2010**, 082 (2010), 1004.5490.
 - [27] J. Dick, F. Y. Kuo, and I. H. Sloan, Acta Numerica **22**, 133 (2013), ISSN 1474-0508, URL http://journals.cambridge.org/article_S0962492913000044.
 - [28] F. Kuo, Journal of Complexity **19**, 301 (2003), ISSN 0885-064X, oberwolfach Special Issue, URL <http://www.sciencedirect.com/science/article/pii/S0885064X03000062>.
 - [29] J. Dick, Journal of Complexity **20**, 493 (2004), ISSN 0885-064X, URL <http://www.sciencedirect.com/science/article/pii/S0885064X04000044>.
 - [30] K. A. Olive et al. (Particle Data Group), Chin. Phys. **C38**, 090001 (2014).
 - [31] T. Hahn, Comput. Phys. Commun. **168**, 78 (2005), hep-ph/0404043.
 - [32] T. Hahn and M. Perez-Victoria, Comput.Phys.Comm. **118**, 153 (1999), hep-ph/9807565.